
DEEP WEAKLY-SUPERVISED ANOMALY DETECTION

A PREPRINT

Guansong Pang

Australian Institute for Machine Learning
University of Adelaide
Adelaide, SA 5005, Australia
guansong.pang@adelaide.edu.au

Chunhua Shen

Australian Institute for Machine Learning
University of Adelaide
Adelaide, SA 5005, Australia
chunhua.shen@adelaide.edu.au

Huidong Jin

Data61
CSIRO
Canberra, ACT 2601, Australia
warren.jin@csiro.au

Anton van den Hengel

Australian Institute for Machine Learning
University of Adelaide
Adelaide, SA 5005, Australia
anton.vandenhengel@adelaide.edu.au

December 25, 2021

ABSTRACT

Anomaly detection is typically posited as an unsupervised learning task in the literature due to the prohibitive cost and difficulty to obtain large-scale labeled anomaly data, but this ignores the fact that a very small number (*e.g.*, a few dozens) of labeled anomalies can often be made available with small/trivial cost in many real-world anomaly detection applications. To leverage such labeled anomaly data, we study an important anomaly detection problem termed *weakly-supervised anomaly detection*, in which, in addition to a large amount of unlabeled data, a limited number of labeled anomalies are available during modeling. Learning with the small labeled anomaly data enables *anomaly-informed* modeling, which helps identify anomalies of interest and address the notorious high false positives in unsupervised anomaly detection. However, the problem is especially challenging, since (i) the limited amount of labeled anomaly data often, if not always, cannot cover all types of anomalies and (ii) the unlabeled data is often dominated by normal instances but has anomaly contamination. We address the problem by formulating it as a pairwise relation prediction task. Particularly, our approach defines a two-stream ordinal regression neural network to learn the relation of randomly sampled instance pairs, *i.e.*, whether the instance pair contains two labeled anomalies, one labeled anomaly, or just unlabeled data instances. The resulting model effectively leverages both the labeled and unlabeled data to substantially augment the training data and learn well-generalized representations of normality and abnormality. Comprehensive empirical results on 40 real-world datasets show that our approach (i) significantly outperforms four state-of-the-art methods in detecting both of the known and previously unseen anomalies and (ii) is substantially more data-efficient.

1 Introduction

Anomaly detection aims at identifying exceptional data instances that have a significant deviation from the majority of data instances, which can offer important insights into broad applications, such as identifying fraudulent transactions or insider trading, detecting network intrusions, and early detection of diseases or adverse drug reactions. Numerous anomaly detection methods have been introduced [1, 2, 3, 4, 5, 6, 7, 8, 9, 10, 11, 12], of which most are unsupervised methods. The popularity of the unsupervised methods is mainly due to that they avoid the prohibitive cost of labeling large-scale anomaly data as required in fully-supervised approaches. However, since they do not have any prior knowledge of the anomalies of interests, many anomalies they identify are often data noises or uninteresting data instances, leading to high false positives or low detection recall. More importantly, although collecting large-scale anomaly data is often too costly (if it is possible), a very small number of labeled anomalies can often be made available

with small/trivial cost in many real-world anomaly detection applications. These labeled anomalies provide some prior knowledge of the anomalies of interests and should be well leveraged to enable more accurate anomaly detection. Those labeled anomaly data may come from a deployed detection system, *e.g.*, a few successfully detected network intrusion records, or they may be from end-users, such as a small number of fraudulent credit card transactions that are reported by bank clients.

To address these aforementioned issues, we study a more practical anomaly detection problem, termed *weakly-supervised anomaly detection*, in which a limited number of labeled anomalies and a large amount of unlabeled data are provided at the training stage. This problem allows us to build anomaly-informed detection models which help identify anomalies of interest and address the notorious high false positive errors in unsupervised anomaly detection [13]. Furthermore, it requires only a very small amount of labeled anomaly data, eliminating the reliance on large-scale and complete labeled anomaly data in fully-supervised approaches.

However, this problem is especially challenging. This is because we have only limited labeled data for the anomaly class, and moreover, anomalies typically stem from unknown events. Therefore, the limited labeled anomalies often, if not always, cannot cover all types of anomalies. As a result, these limited anomalies can only provide incomplete supervision information, and thus, one significant challenge here is to generalize from these limited incomplete labeled anomaly data to detect *known anomalies* (*i.e.*, anomalies that demonstrate similar abnormal behaviors to the labeled anomalies) and *unknown anomalies* (*i.e.*, new types of anomalies that are unknown during training). Another main challenge lies on the difficulty of leveraging the large unlabeled data that is often dominated by normal instances but has anomaly contamination.

To address the proposed problem, this paper introduces a novel anomaly detection formulation and its instantiation, namely Pairwise Relation prediction-based ordinal regression Network (PReNet). Particularly, the problem is formulated as a *surrogate* supervised learning task, of which a *two-stream ordinal regression neural network* is defined to predict the relation of randomly sampled instance pairs, *i.e.*, to discriminate whether a instance pair contains two labeled anomalies, only one labeled anomaly, or just unlabeled instances. To achieve this goal, PReNet first generates pairs of instances sampled from the small labeled anomaly data and the large unlabeled data, and then augments the pairs with a *synthetic ordinal class* feature, in which a large *scalar* value for the instance pairs with two labeled anomalies, and an intermediate value for the pairs with one labeled anomaly and one unlabeled instance, and a small value for the other pairs with unlabeled instances are assigned. PReNet further feeds these pairwise samples into the two-stream regression network to minimize the differences between the regression predictions and the synthetic ordinal labels. The model is therefore optimized to output larger prediction scores for the input pairs that contain two anomalies than the pairs with one anomaly or none. By doing so, the prediction scores can be inherently defined as the anomaly scores of the pairs. In other words, PReNet simultaneously optimizes the pairwise relation prediction and anomaly score learning. At the testing/detecting stage, PReNet pairs a new instance with the training instances and uses the regression network to infer its anomaly score.

There have been a few early explorations in this research line using traditional methods [14, 15, 16] or recently emerged deep anomaly detection methods¹ [9], but they leverage the labeled anomalies as auxiliary data to enhance an existing anomaly measure or perform a classification-based anomaly detection. This may lead to insufficient exploitation of the labeled data and/or poor generalization. Our very recent work [11] is the most relevant work, in which a method called deviation network (DevNet) is introduced to leverage the few labeled anomalies and unlabeled data to learn binary representations of normality and abnormality. It is done by enforcing the anomaly scores of individual data instances to fit a one-sided Gaussian distribution, achieving significant improvement over current state-of-the-arts. PReNet is motivated by the success of DevNet, but they represent two completely different approaches. DevNet leverages the Gaussian prior to learn the anomaly scores and it may fail to work when the prior is inexact, whereas PReNet learns the anomaly scores by ordinal regression and does not involve any probability distribution assumption over the anomaly scores, enabling PReNet to learn more faithful representations than DevNet. Furthermore, the pairwise relation prediction substantially augments the labeled data and enables PReNet to learn multifaceted representations of normality and abnormality other than the binary representations in DevNet, resulting in substantially better generalization ability.

Additionally, note that well established semi-supervised anomaly detection [18, 19, 20] focuses on learning patterns of the normal class using *large labeled normal data*. By contrast, the weakly-supervised setting here is to take full advantage of *limited (often incomplete) labeled anomaly data* to learn detection models that are highly generalized to detect both the known and unknown anomalies. As a result, these two problems are fundamentally different in terms of the given data and the nature of the problem. These differences are summarized in Table 1. On the other hand, the term ‘weakly-supervised’ is also intentionally used to emphasize the nature of the scarceness and incompleteness of the available labeled anomalies in our setting.

¹Deep anomaly detection methods refer to any methods that exploit deep learning techniques [17] to learn feature representations or anomaly scores for anomaly detection.

Table 1: Weakly- and Semi-supervised Anomaly Detection Settings

Approach	Training Data	Problem
Semi-supervised	Large <i>labeled normal data</i> and unlabeled data	Learn patterns of labeled normal data
Weakly-supervised	<i>Limited labeled anomaly data</i> , large unlabeled data	Learn to generalize from a few labeled known anomalies to detect both known and unknown anomalies

In summary, this work makes the following four main contributions.

- We propose a novel formulation for synthesizing pairing-based data augmentation and ordinal regression to achieve deep weakly-supervised anomaly detection via ‘supervised’ pairwise relation learning. This approach substantially augments the labeled data and learns *anomaly-informed* detection models with desired *generalizability*.
- A novel method, namely PReNet, is instantiated from our formulation to simultaneously learn the pairwise relations and anomaly scores by training a two-stream ordinal regression neural network, achieving *data-efficient* learning and well-generalized models to detect known and unknown anomalies.
- We theoretically and empirically show that our two-stream ordinal regression network can effectively leverage the large unlabeled data while being tolerant to small anomaly contamination.
- As a result, we show by our empirical results on 40 real-world datasets, including 12 datasets that contain known anomalies and 28 datasets that contain exclusively unknown anomalies, that PReNet (i) significantly outperforms four state-of-the-art competing methods in detecting both known and unknown anomalies, *e.g.*, achieving 10%-30% improvement in precision-recall rates in detecting unknown anomalies, and (ii) obtains a substantially better data efficiency, *e.g.*, it requires 50%-87.5% less labeled anomalies to perform comparably well to, or substantially better than, the best contenders.

2 Learning Anomaly Scores by Predicting Pairwise Relation

2.1 Problem Formulation

Given a training dataset $\mathcal{X} = \{\mathbf{x}_1, \mathbf{x}_2, \dots, \mathbf{x}_N, \mathbf{x}_{N+1}, \dots, \mathbf{x}_{N+K}\}$ of size $N + K$, with $\mathbf{x}_i \in \mathbb{R}^D$, where $\mathcal{U} = \{\mathbf{x}_1, \mathbf{x}_2, \dots, \mathbf{x}_N\}$ is a large unlabeled dataset and $\mathcal{A} = \{\mathbf{x}_{N+1}, \mathbf{x}_{N+2}, \dots, \mathbf{x}_{N+K}\}$ with $K \ll N$ is a very small set of labeled anomalies that provide some prior knowledge of anomalies, our goal is to learn an anomaly scoring function $\phi : \mathcal{X} \mapsto \mathbb{R}$ that assigns anomaly scores to data instances in a way that we have $\phi(\mathbf{x}_i) > \phi(\mathbf{x}_j)$ if \mathbf{x}_i is an anomaly and \mathbf{x}_j is a normal data instance.

To obtain more labeled data and effectively leverage both the small labeled anomalies and large unlabeled data, we formulate the problem as a pairwise relation learning task, of which we learn to discriminate three types of *unordered* random instance pairs, including anomaly-anomaly pair, anomaly-unlabeled pair, unlabeled-unlabeled pair. More importantly, since our primary goal is to learn anomaly scores, we aim to unify the relation learning and anomaly scoring such that the learner assigns substantially larger anomaly scores to the data instance pairs that contain anomalies than the other instance pairs. This can be achieved by formulating the relation learning task as an ordinal regression task. Specifically, let $\mathcal{P} = \{\{\mathbf{x}_i, \mathbf{x}_j, y_{ij}\} \mid \mathbf{x}_i, \mathbf{x}_j \in \mathcal{X} \text{ and } y_{ij} \in \mathbb{N}\}$ be a set of pairs of randomly sampled instances with artificial class labels, where each pair $\{\mathbf{x}_i, \mathbf{x}_j\}$ has one of the three pairwise relations: $C_{\{\mathbf{a}, \mathbf{a}\}}$, $C_{\{\mathbf{a}, \mathbf{u}\}}$ and $C_{\{\mathbf{u}, \mathbf{u}\}}$ ($\mathbf{a} \in \mathcal{A}$ and $\mathbf{u} \in \mathcal{U}$) and $\mathbf{y} \in \mathbb{N}^{|\mathcal{P}|}$ is an ordinal class feature with *decreasing* value assignments to the respective $C_{\{\mathbf{a}, \mathbf{a}\}}$, $C_{\{\mathbf{a}, \mathbf{u}\}}$ and $C_{\{\mathbf{u}, \mathbf{u}\}}$ pairs, *i.e.*, $y_{\{\mathbf{a}, \mathbf{a}\}} > y_{\{\mathbf{a}, \mathbf{u}\}} > y_{\{\mathbf{u}, \mathbf{u}\}}$, then the pairwise relations and anomaly scores are simultaneously learned by training a *ternary* ordinal regression function $\phi : \mathcal{P} \mapsto \mathbb{R}$.

2.2 The Instantiated Model: PReNet

Our deep anomaly detection method PReNet is then instantiated from the formulation, which simultaneously learns pairwise relations and anomaly scores by training an end-to-end ordinal regression neural network. As shown in Fig. 1, PReNet consists of three modules: pairing data augmentation, end-to-end anomaly score learner and ordinal regression. The data augmentation generates the instance pair set \mathcal{P} . The relation learning (anomaly scoring) function ϕ is a composition of a feature learner ψ and a relation (anomaly score) learner η , which can be trained in an end-to-end manner with an ordinal regression loss function.

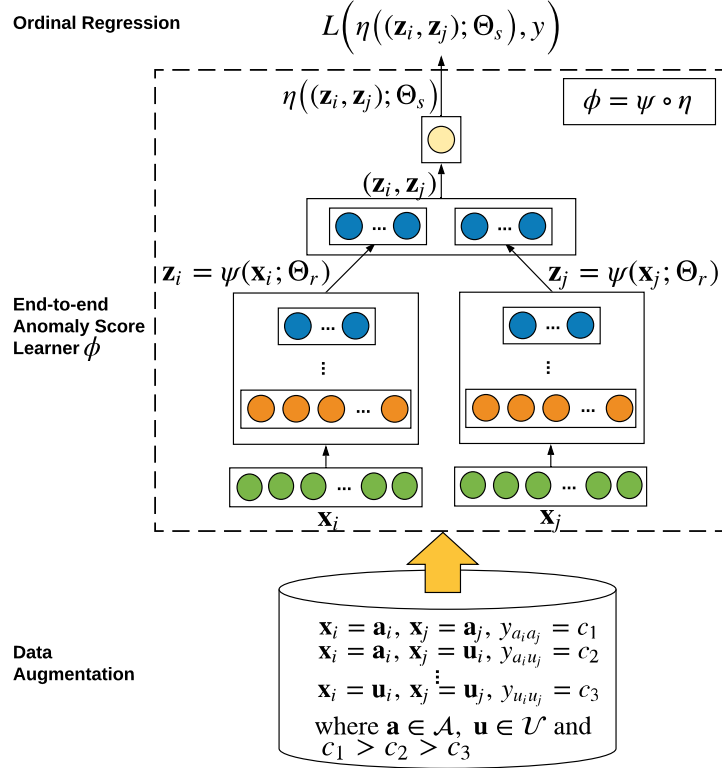


Figure 1: PReNet - Pairwise Relation prediction-based ordinal regression Network. It takes $C_{\{a,a\}}$, $C_{\{a,u\}}$ and $C_{\{u,u\}}$ instance pairs as inputs and learns to discriminate the three types of pairwise relations while at the same time yielding *decreasing* prediction scores to the respective $C_{\{a,a\}}$, $C_{\{a,u\}}$ and $C_{\{u,u\}}$ instance pairs. These prediction scores are inherently coupled with the discrimination of anomalies and normal instances and thus can be used as anomaly scores.

2.2.1 Data Augmentation by Pairing

Different from popular editing-based augmentation [21, 22], a two-step pairing-based data augmentation method is used for our problem to substantially extend the labeled data: (i) we first generate a set of instance pairs with instances randomly sampled from the small labeled anomaly set \mathcal{A} and the large unlabeled dataset \mathcal{U} , and categorize the pairs into three classes $C_{\{a,a\}}$, $C_{\{a,u\}}$ and $C_{\{u,u\}}$ based on the sources that the instances of each pair sample from, where $\mathbf{a} \in \mathcal{A}$ and $\mathbf{u} \in \mathcal{U}$; and (ii) a synthetic ordinal class feature \mathbf{y} is then added, in which the instance pairs of the three classes are assigned with *scalar* class labels, such that $y_{\{a,a\}} = c_1$, $y_{\{a,u\}} = c_2$, $y_{\{u,u\}} = c_3$ and $c_1 > c_2 > c_3 \geq 0$. By doing so, we efficiently synthesize \mathcal{A} and \mathcal{U} to produce a large fully labeled dataset $\mathcal{P} = \{\{\mathbf{x}_i, \mathbf{x}_j, y_{ij}\} \mid \mathbf{x}_i, \mathbf{x}_j \in \mathcal{X} \text{ and } y_{ij} \in \mathbb{N}\}$.

More importantly, \mathcal{P} contains critical information for discriminating anomalies from normal data instances. This is due to the fact that, as anomalies are rare data instances, the unlabeled dataset \mathcal{U} is often dominated by normal data instances. As a result, most $C_{\{u,u\}}$ pairs consist of normal instances only. Thus, with \mathcal{P} as data inputs, PReNet is fed with training samples that contain key information for discriminating anomalies and normal instances, since $C_{\{a,a\}}$, $C_{\{a,u\}}$ and $C_{\{u,u\}}$ are approximately anomaly-anomaly, anomaly-normal and normal-normal pairs. Note that a few $C_{\{a,u\}}$ and $C_{\{u,u\}}$ pairs may contain some noisy pairs from this aspect due to potential anomaly contamination in \mathcal{U} , but we found theoretically and empirically that PReNet is generally robust to these noisy pairs (see Sections 3.2 and 4.7.1 for detail).

2.2.2 End-to-end Anomaly Score Learner

An end-to-end anomaly score (or pairwise relation) learner is then defined to take pairs of data instances as inputs and directly output the anomaly scores of the pairs. Let $\mathcal{Z} \in \mathbb{R}^M$ be an intermediate representation space, we define a two-stream anomaly scoring network $\phi((\cdot, \cdot); \Theta) : \mathcal{P} \mapsto \mathbb{R}$ as a composition of a feature learner $\psi(\cdot; \Theta_r) : \mathcal{X} \mapsto \mathcal{Z}$ and an anomaly scoring function $\eta((\cdot, \cdot); \Theta_s) : (\mathcal{Z}, \mathcal{Z}) \mapsto \mathbb{R}$, where $\Theta = \{\Theta_r, \Theta_s\}$. Specifically, $\psi(\cdot; \Theta_r)$ is a neural

feature learner with $H \in \mathbb{N}$ hidden layers and weight matrices $\Theta_r = \{\mathbf{W}^1, \mathbf{W}^2, \dots, \mathbf{W}^H\}$:

$$\mathbf{z} = \psi(\mathbf{x}; \Theta_r), \quad (1)$$

where $\mathbf{x} \in \mathcal{X}$ and $\mathbf{z} \in \mathcal{Z}$. Different network structures can be used here, such as multilayer perceptrons for multidimensional data, convolutional networks for image data, or recurrent networks for sequence data [17].

$\eta((\cdot, \cdot); \Theta_s)$ is defined as an *anomaly score learner* which uses a linear neural unit in the output layer to compute the anomaly scores based on the intermediate representations:

$$\eta((\mathbf{z}_i, \mathbf{z}_j); \Theta_s) = \sum_{k=1}^M w_k^o z_{ik} + \sum_{l=1}^M w_{M+l}^o z_{jl} + w_{2M+1}^o, \quad (2)$$

where $\mathbf{z} \in \mathcal{Z}$, $(\mathbf{z}_i, \mathbf{z}_j)$ is a *concatenation* operation of \mathbf{z}_i and \mathbf{z}_j , and $\Theta_s = \{\mathbf{w}^o\}$, in which $\{w_1^o, w_2^o, \dots, w_{2M}^o\}$ are weight parameters and w_{2M+1}^o is a bias term. As shown in Fig. 1, to reduce the optimization complexity, PReNet uses a two-stream network with the shared weight parameters Θ_r to learn the representations \mathbf{z}_i and \mathbf{z}_j .

Lastly $\phi((\cdot, \cdot); \Theta)$ can be formally represented as

$$\phi((\mathbf{x}_i, \mathbf{x}_j); \Theta) = \eta((\psi(\mathbf{x}_i; \Theta_r), \psi(\mathbf{x}_j; \Theta_r)); \Theta_s), \quad (3)$$

which can be trained in an end-to-end fashion to directly map data inputs to scalar scores.

Note that the concatenation results in an *ordered* pair $(\mathbf{z}_i, \mathbf{z}_j)$. This does not affect the unordered pairs from the $C_{\{\mathbf{a}, \mathbf{a}\}}$ and $C_{\{\mathbf{u}, \mathbf{u}\}}$ classes since the instances of these pairs come from the same dataset (*i.e.*, \mathcal{A} or \mathcal{U}), but it may produce inverse effects on our training with the $C_{\{\mathbf{a}, \mathbf{u}\}}$ pairs. This problem can be simply addressed by organizing all unordered $C_{\{\mathbf{a}, \mathbf{u}\}}$ pairs into ordered pairs $C_{(\mathbf{a}, \mathbf{u})}$ before training.

2.2.3 Ordinal Regression

PReNet then feeds the ordinal class labels and the anomaly scores yielded by ϕ to optimize the scores using an ordinal regression objective, *i.e.*, minimizing the difference between the prediction scores and the ordinal labels $y_{\{\mathbf{a}, \mathbf{a}\}}$, $y_{\{\mathbf{a}, \mathbf{u}\}}$ and $y_{\{\mathbf{u}, \mathbf{u}\}}$. It is equivalent to assigning larger prediction scores to the $C_{\{\mathbf{a}, \mathbf{a}\}}$ and $C_{\{\mathbf{a}, \mathbf{u}\}}$ instance pairs than the $C_{\{\mathbf{u}, \mathbf{u}\}}$ instance pairs. Our loss is defined as below to guide the optimization:

$$L(\phi((\mathbf{x}_i, \mathbf{x}_j); \Theta), y_{ij}) = |y_{ij} - \phi((\mathbf{x}_i, \mathbf{x}_j); \Theta)|. \quad (4)$$

The absolute prediction error, instead of square error, is used in the loss to reduce the effect of potential noisy pairs due to the anomaly contamination in \mathcal{U} . The three class labels $y_{\{\mathbf{a}, \mathbf{a}\}} = 8$, $y_{\{\mathbf{a}, \mathbf{u}\}} = 4$ and $y_{\{\mathbf{u}, \mathbf{u}\}} = 0$ are used by default to enforce large margins among the anomaly scores of the three types of instance pairs. PReNet also works very well with other value assignments as long as there are reasonably large margins among the ordinal class labels. Therefore, the overall objective function can be written as

$$\arg \min_{\Theta} \frac{1}{|\mathcal{B}|} \sum_{\{\mathbf{x}_i, \mathbf{x}_j, y_{ij}\} \in \mathcal{B}} |y_{ij} - \phi((\mathbf{x}_i, \mathbf{x}_j); \Theta)| + \lambda R(\Theta), \quad (5)$$

where \mathcal{B} is a sample batch from \mathcal{P} and $R(\Theta)$ is a regularization term with the hyperparameter λ . The detailed optimization settings are provided in Section 4.2.

2.3 Anomaly Detection Using PReNet

2.3.1 Training Stage

Algorithm 1 presents the procedure of training PReNet. Step 1 first extends the data \mathcal{X} into a set of instance pairs with ordinal class labels, \mathcal{P} . After an uniform *Glorot* weight initialization [23] in Step 2, PReNet performs stochastic gradient descent (SGD) based optimization to learn Θ in Steps 3-9 and obtains the optimized ϕ in Step 10. Particularly, stratified random sampling is used in Step 5 to ensure the sample balance of the three classes in \mathcal{B} , *i.e.*, for each batch $\frac{|\mathcal{B}|}{2}$ instance pairs are sampled from the $C_{\{\mathbf{u}, \mathbf{u}\}}$ class and $\frac{|\mathcal{B}|}{4}$ instance pairs are respectively sampled from the $C_{\{\mathbf{a}, \mathbf{a}\}}$ and $C_{\{\mathbf{a}, \mathbf{u}\}}$ classes. This is equivalent to oversampling the two anomaly-related classes, $C_{\{\mathbf{a}, \mathbf{a}\}}$ and $C_{\{\mathbf{a}, \mathbf{u}\}}$, to avoid bias towards the $C_{\{\mathbf{u}, \mathbf{u}\}}$ class due to the class-imbalance problem. Step 6 performs the forward propagation of the network and computes the loss. Step 7 then uses the loss to perform gradient descent steps.

Algorithm 1 *Training PReNet*

Input: $\mathcal{X} \in \mathbb{R}^D$ with $\mathcal{X} = \mathcal{U} \cup \mathcal{A}$ and $\emptyset = \mathcal{U} \cap \mathcal{A}$
Output: $\phi : (\mathcal{X}, \mathcal{X}) \mapsto \mathbb{R}$ - an anomaly score mapping

- 1: $\mathcal{P} \leftarrow$ Augment the training data with \mathcal{U} and \mathcal{A}
- 2: Randomly initialize Θ
- 3: **for** $i = 1$ to n_epochs **do**
- 4: **for** $j = 1$ to $n_batches$ **do**
- 5: $\mathcal{B} \leftarrow$ Randomly sample b data instance pairs from \mathcal{P}
- 6: $loss \leftarrow \frac{1}{b} \sum_{\{\mathbf{x}_i, \mathbf{x}_j, y_{ij}\} \in \mathcal{B}} |y_{ij} - \phi((\mathbf{x}_i, \mathbf{x}_j); \Theta)| + \lambda R(\Theta)$
- 7: Perform a gradient descent step w.r.t. the parameters in Θ
- 8: **end for**
- 9: **end for**
- 10: **return** ϕ

2.3.2 Anomaly Scoring Stage

At the testing stage, given a test instance \mathbf{x}_k , PReNet first pairs it with data instances randomly sampled from \mathcal{A} and \mathcal{U} , and then defines its anomaly score as

$$s_{\mathbf{x}_k} = \frac{1}{2E} \left[\sum_{i=1}^E \phi((\mathbf{a}_i, \mathbf{x}_k); \Theta^*) + \sum_{j=1}^E \phi((\mathbf{x}_k, \mathbf{u}_j); \Theta^*) \right], \quad (6)$$

where Θ^* are the parameters of a trained ϕ , and \mathbf{a}_i and \mathbf{u}_j are randomly sampled from the respective \mathcal{A} and \mathcal{U} . $s_{\mathbf{x}_k}$ can be interpreted as an ensemble of the anomaly scores of a set of \mathbf{x}_k -oriented pairs. Due to the loss in Eqn. (4), $s_{\mathbf{x}_k}$ is optimized to be greater than $s_{\mathbf{x}'_k}$ given \mathbf{x}_k is an anomaly and \mathbf{x}'_k is a normal instance. The ensemble scores are employed to achieve stable anomaly scoring. PReNet can perform very stably as long as the ensemble size E is sufficiently large due to the law of large numbers ($E = 30$ is used by default).

3 Theoretical Foundation of PReNet

The performance of the proposed weakly-supervised learning framework and the PReNet algorithm are based on two reasonable assumptions. The first one is that all the labeled anomalies are true anomalies. The second one is that the proportion of true anomalies in the unlabeled data instances is relatively small. The performance of PReNet may drop on data sets where neither assumptions is held.

3.1 Transformative Data Augmentation

The underlying purpose of our data augmentation is to leverage both the limited labeled anomaly data and large unlabeled data by transferring a highly imbalanced weakly-supervised anomaly detection problem to a large balanced supervised learning of pairwise relations. First, due to the random sampling of pairwise relations used in PReNet, the sample size of the training data theoretically increases from $N + K$ for the weakly-supervised anomaly detection problem to $K^3 N^3$ for the pairwise relation learning, which enables deep learning even for an anomaly detection problem with only a few thousands of unlabeled instances and dozens of labeled anomalies. We have K^2 of $C_{\{\mathbf{a}, \mathbf{a}\}}$ pairwise relations, $K \times N$ of $C_{\{\mathbf{a}, \mathbf{u}\}}$ and N^2 of $C_{\{\mathbf{u}, \mathbf{u}\}}$ relations; in Step 5 of PReNet in Algorithm 1, we independently sample from three different pairwise relations, and thus, there are $K^3 N^3$ pairwise relations to choose from. Such a large size clearly helps build up the generalizability and then the detection performance of our anomaly detection model. Note that PReNet uses a shared-weight two-stream network in its representation learner $\psi(\cdot; \Theta_r)$, so the representation learning is still optimized on the original \mathcal{X} data space rather than the pairwise higher-order \mathcal{P} space. This trick well supports the scale-up of the training sample size while adding nearly no extra model complexity.

Furthermore, in Step 5 of PReNet, we sample about a quarter of pairwise relations from $C_{\{\mathbf{a}, \mathbf{a}\}}$, a quarter from $C_{\{\mathbf{a}, \mathbf{u}\}}$, and half from $C_{\{\mathbf{u}, \mathbf{u}\}}$. That means, about half of data instances in these pairwise relations are from labeled anomalies. Through oversampling pairwise relations from $C_{\{\mathbf{a}, \mathbf{a}\}}$ and $C_{\{\mathbf{a}, \mathbf{u}\}}$, labeled anomalies are relatively balanced with unlabeled data instances, during the ‘supervised’ anomaly score learning in Steps 5 and 6. Thus, the imbalance issue caused by $K \ll N$, which often substantially deteriorates learning performance, is massaged.

More importantly, the pairwise interaction between the pair samples of $C_{\{\mathbf{a}, \mathbf{a}\}}$ or $C_{\{\mathbf{a}, \mathbf{u}\}}$ carries diverse information from each other, and the corresponding pairwise data space is significantly larger than that of the small labeled anomaly

set \mathcal{A} . Thus, oversampling from these two pairwise sample pools substantially augments our training data with naturally diverse and discriminative pairwise anomaly-related samples, providing substantially richer anomaly supervision information than oversampling from the small anomaly set \mathcal{A} only.

This augmented data enables significantly improved generalizability in detecting both known and unknown anomalies. Additionally, the ternary ordinal regression enables PReNet to learn the representations of respective anomaly-anomaly, anomaly-normal and normal-normal interactions; and Eqn. (6) considers every two possible combination of these three types of representations to infer anomaly scores. That means PReNet performs anomaly scoring using a collective energy of two-level hierarchical representations, *i.e.*, representations of $C_{\{\mathbf{a},\mathbf{a}\}}$, $C_{\{\mathbf{a},\mathbf{u}\}}$ and $C_{\{\mathbf{u},\mathbf{u}\}}$ and their pairwise combinations. This enables PReNet to spot the abnormality from multiple different aspects. PReNet can therefore identify subtle or unknown anomalies when their pairwise interaction with training instances demonstrate similar patterns to the anomaly-anomaly/normal relations, or deviated patterns from the anomaly/normal-normal relations.

3.2 End-to-end Anomaly Score Optimization with Ordinal Regression

We assume the proportion of true anomalies in the unlabeled data instances, ϵ , is small, say $\leq 5\%$, which is normally the case in real-world applications [13]. Based on randomly sampling, we can obtain the expectation of the pairwise relation proportions in each batch \mathcal{B} in Step 5 of PReNet in Algorithm 1. Specifically, there are $\frac{1}{4} + \frac{1}{4}\epsilon + \frac{1}{2}\epsilon^2$ from true anomaly-anomaly pairwise relations, and $\frac{1}{4} + \frac{3}{4}\epsilon - \epsilon^2$ from true anomaly-normal pairwise relations, and $\frac{1}{2} - \epsilon + \frac{1}{2}\epsilon^2$ from normal-normal pairwise relations. Thus, a small percentage of the pairwise relations, $2\epsilon - \epsilon^2$, could have mis-assigned ordinal labels during the data augmentation procedure. Considering the tolerance of the regression performance to these outliers [24, 25], PReNet can perform well when the proportion of true anomalies in the unlabeled data instances is reasonably small, say $\leq 5\%$. With the recent development of regression techniques [25], the breakdown point of modern robust regression techniques could reach as large as 50%, *e.g.*, through reaching a nice tradeoff iteratively between the regularization term and the loss term [24]. Breakdown point is to measure the proportion of anomalies that a regression estimate can tolerate before it goes to infinity. That means the proposed technique may have potential to tolerate ϵ around 25%. We will leave realizing the full potential to future work, though our experimental results in Section 4.7.1 will illustrate the reliable performance of the proposed PReNet to different level of noises in the unlabeled data.

On the other hand, from the regression modeling, we have expectation for different type of pairwise relations for true anomaly \mathbf{a}_k and normal data instance \mathbf{n}_l :

$$\begin{aligned}\mathbb{E}[\phi((\mathbf{a}_i, \mathbf{a}_k); \Theta^*)] &= c_1, \\ \mathbb{E}[\phi((\mathbf{a}_k, \mathbf{u}_j); \Theta^*)] &= c_2, \\ \mathbb{E}[\phi((\mathbf{a}_i, \mathbf{n}_l); \Theta^*)] &= \mathbb{E}[\phi((\mathbf{a}_i, \mathbf{u}_j); \Theta^*)] - \epsilon \mathbb{E}[\phi((\mathbf{a}_i, \mathbf{a}_j); \Theta^*)] \\ &= c_2 - \epsilon c_1, \\ \mathbb{E}[\phi((\mathbf{n}_l, \mathbf{u}_j); \Theta^*)] &= \mathbb{E}[\phi((\mathbf{u}_i, \mathbf{u}_j); \Theta^*)] - \epsilon \mathbb{E}[\phi((\mathbf{a}_i, \mathbf{u}_j); \Theta^*)] \\ &= c_3 - \epsilon c_1.\end{aligned}$$

Thus, from Eqn. (6), we have

$$\begin{aligned}\mathbb{E}[s_{\mathbf{x}_k} | \mathbf{x}_k \text{ is an anomaly}] &= \frac{1}{2E} \left\{ E \times \mathbb{E}[\phi((\mathbf{a}_i, \mathbf{a}_k); \Theta^*)] \right. \\ &\quad \left. + E \times \mathbb{E}[\phi((\mathbf{a}_k, \mathbf{u}_j); \Theta^*)] \right\} = \frac{c_1 + c_2}{2},\end{aligned}\quad (7)$$

and

$$\begin{aligned}\mathbb{E}[s_{\mathbf{x}_k} | \mathbf{x}_k \text{ is normal}] &= \frac{1}{2E} \left\{ E \times \mathbb{E}[\phi((\mathbf{a}_i, \mathbf{n}_l); \Theta^*)] \right. \\ &\quad \left. + E \times \mathbb{E}[\phi((\mathbf{n}_l, \mathbf{u}_j); \Theta^*)] \right\} = \frac{c_2 + c_3 - 2\epsilon c_1}{2}.\end{aligned}\quad (8)$$

As $c_1 > c_2 > c_3 \geq 0$, $\frac{c_1 + c_2}{2} > \frac{c_2 + c_3 - 2\epsilon c_1}{2}$ for small ϵ . That means PReNet is optimized in an end-to-end fashion to guarantee that a true anomaly is expected to have a larger anomaly score than normal data instances when the anomaly contamination in the unlabeled data is small.

4 Experiments

We aim to empirically examine the following four questions:

- **Detection of both known and unknown anomalies.** Can PReNet generalize from a limited number of labeled anomalies to effectively detect both the known and unknown anomalies in real-world datasets?
- **Effectiveness of leveraging the limited labeled data.** How effective is PReNet in learning detection models with different amount of labeled data?
- **Tolerance to Anomaly Contamination.** How tolerant is PReNet to the anomaly contamination in the unlabeled data?
- **Importance of each individual component of PReNet.** How does each individual component of PReNet contribute to the overall performance of PReNet?

4.1 Datasets

To explicitly evaluate the performance of detecting known and unknown anomalies, we separate our datasets into two groups, including one group contains 12 datasets used for detection of known anomalies and another group contains 28 datasets designed to exclusively evaluate the performance of detecting unknown anomalies.

As shown in Table 2, 12 widely-used publicly available real-world datasets² are used for detection of known anomalies, which are from diverse domains, *e.g.*, intrusion detection, fraud detection, and disease detection [26, 5, 11]. Specifically, the *donors* data is taken from KDD Cup 2014 for predicting excitement of donation projects, with exceptionally exciting projects used as anomalies (6.0% of all data instances). The *census* data is extracted from the US census bureau database, in which we aim to detect the rare high-income persons (6.0%). *fraud* is for fraudulent credit card transaction detection, with fraudulent transactions (0.2%) as anomalies. *celeba* contains more than 200K celebrity images, each with 40 attribute annotations. We use the bald attribute as our detection target, in which the scarce bald celebrities (3.0%) are treated as anomalies and the other 39 attributes form the feature space. The *DoS*, *reconnaissance*, *fuzzers* and *backdoor* datasets are derived from a popular intrusion detection dataset called *UNSW-NB15* [26] with the respective DoS (15.0%), reconnaissance (13.1%), fuzzers (3.1%) and backdoor (2.4%) attacks as anomalies against the ‘normal’ class. *w7a* is a web page classification dataset, with the minority classes (3.0%) as anomalies. *campaign* is a dataset of bank marketing campaigns, with rarely successful campaigning records (11.3%) as anomalies. *news20* is one of the most popular text classification corpora, which is converted into anomaly detection data via random downsampling of the minority class (5.0%) based on [5, 27]. *thyroid* is for disease detection, in which the anomalies are the hypothyroid patients (7.4%). Seven of these datasets contain real anomalies, including *donors*, *fraud*, *DoS*, *reconnaissance*, *fuzzers*, *backdoor* and *thyroid*. The other five datasets contain semantically real anomalies, *i.e.*, they are rare and very different from the majority of data instances. So, they serve as a good testbed for the evaluation of anomaly detection techniques.

To replicate the real-world scenarios where we have a few labeled anomalies and large unlabeled data, we first have a stratified split of the anomalies and normal instances into two subsets, with 80% data as training data and the other 20% data as holdup test set. Since the unlabeled data is often anomaly-contaminated, we then combine some randomly selected anomalies with the whole normal training data instances to form the unlabeled dataset \mathcal{U} . We further randomly sample a limited number of anomalies from the anomaly class to form the labeled anomaly set \mathcal{A} .

Table 3 presents the 28 datasets for the evaluation of detecting unknown anomalies. These datasets are derived from the above four intrusion attack datasets *DoS*, *reconnaissance*, *fuzzers* and *backdoor*, with data instances spanned by the same feature space. To guarantee that the evaluation data contains unknown anomalies only, the anomaly class in one of these four datasets is held up for evaluation, while the anomalies in any combinations of the remaining three datasets are combined to form the pool of known anomalies. The type of the holdup anomalies is always different from that in the anomaly pool and can be safely treated as unknown anomalies. We have 28 possible permutations under this setting, resulting in 28 datasets with different known and/or unknown anomalies. For the training, \mathcal{A} contains the anomalies sampled from the known anomalies pool, while the evaluation data is composed of the holdup unknown anomaly class and the 20% holdup normal instances.

4.2 Competing Methods and Parameter Settings

PReNet is compared with the following state-of-the-art methods from four relevant areas:

- DevNet [11]. DevNet is a deep weakly-supervised anomaly detection method that uses a Gaussian prior to directly learn the anomaly scores.

²*donors* and *fraud* are publicly available at <https://www.kaggle.com/>, *w7a* and *news20* are available at <https://www.csie.ntu.edu.tw/~cjlin/libsvmtools/datasets/>, *DoS*, *reconnaissance*, *fuzzers*, *backdoor* are available at <https://www.unsw.adfa.edu.au/unsw-canberra-cyber/cybersecurity/ADFA-NB15-Datasets/>, *celeba* is at <http://mmlab.ie.cuhk.edu.hk/projects/CelebA.html>, and the other datasets are accessible at <https://archive.ics.uci.edu/ml/datasets/>.

- Deep support vector data description (DSVDD) [10]. DSVDD performs support vector data description-based one-class classification with neural networks. The original DSVDD is unsupervised and cannot make use of the labeled anomalies. We adapted it based on [28] to enforce a large margin between the one-class center and the labeled anomalies while minimizing the center-oriented hypersphere. This adaption enhances DSVDD by over 30% accuracy.
- Prototypical network [29]. Prototypical network is a well-known few-shot classification method (denoted as FSNet here), which learns prototypical representations of each class and perform classification based on the distance to the prototypes. We adapt it to our problem by learning respective prototypical representations of the labeled anomalies and the unlabeled data.
- iForest [5]. iForest is a state-of-the-art unsupervised anomaly detection method that calculates the anomaly scores based on how many steps are required to isolate the data points by random half-space partition.

Since our experiments focus on unordered multidimensional data, multilayer perceptron networks are used. Similar to our findings in [9, 11], we empirically found that all deep methods using an architecture with one hidden layer perform better and more stably than using two or more hidden layers. This may be due to the limit of the available labeled data. Following DevNet, one hidden layer with 20 neural units is used in all deep methods. The ReLU activation function $g(a) = \max(0, a)$ is used. An ℓ_2 -norm regularizer with the hyperparameter setting $\lambda = 0.01$ is applied to avoid overfitting. The RMSprop optimizer with the learning rate 0.001 is used. All deep detectors are trained using 50 epochs, with 20 batches per epoch. The batch size is probed in $\{8, 16, 32, 64, 128, 256, 512\}$. The best fits, 512 in PReNet, DevNet and DSVDD, 256 in FSNet, are used by default. Oversampling is applied to the labeled anomaly set \mathcal{A} to well train the deep detection models of DevNet, DSVDD and FSNet.

4.3 Performance Evaluation Metrics

Each detector yields a ranking of data instances based on the anomaly scores. Two popular and complementary metrics, the Area Under Receiver Operating Characteristic Curve (AUC-ROC) and Area Under Precision-Recall Curve (AUC-PR) [30], are calculated based on the anomaly ranking. AUC-ROC summarizes the ROC curve of true positives against false positives, which often presents an overoptimistic view of the detection performance due to the class-imbalance nature of anomaly detection data; whereas AUC-PR is a summarization of the curve of precision and recall w.r.t. the anomalies, which focuses on the performance on the anomaly class only and is often more practical. Larger AUC-ROC (AUC-PR) indicates better performance. The reported AUC-ROC and AUC-PR are averaged results over 10 independent runs. The paired *Wilcoxon* signed rank [31] using the averaged AUC-ROC (AUC-PR) across multiple datasets (*i.e.*, 12 datasets for known anomalies and 28 datasets for unknown anomalies) is used to examine the statistical significance of the performance of PReNet against its competing methods.

4.4 Detection of Known Anomalies

Experiment Settings. We first evaluate the effectiveness of PReNet on the 12 real-world datasets with known anomalies. A consistent anomaly contamination rate and amount of labeled anomalies, is used across all datasets to gain insights into the performance in different real-life applications. Since anomalies are typically rare instances, the anomaly contamination rate is set to 2% by default. The number of labeled anomalies available per data is set to 60, *i.e.*, $|\mathcal{A}| = 60$. We provide the results of PReNet on datasets with different amount of labeled data and anomaly contamination rates later in respective Sections 4.6 and 4.7.1.

Results. The AUC-PR and AUC-ROC results of PReNet and its four competing methods on the 12 datasets are shown in Table 2. PReNet performs significantly better than, or comparably well to, all competing methods in both metrics across the 12 datasets. In terms of AUC-PR performance, on average, PReNet improves all four competing methods by a large margin, *i.e.*, DevNet (3.7%), DSVDD (19.6%), FSNet (54.0%) and iForest (331.1%), which are all statistically significant at the 95% confidence level according to the *Wilcoxon* signed rank test results. Particularly, compared to the top two competing methods, PReNet significantly outperforms DevNet on six datasets, with improvement ranging from 3%-6% on *census*, *backdoor*, *news20* and *thyroid* up to 10%-20% on *campaign* and *w7a*, and they perform comparably well on the rest of six datasets; PReNet performs significantly better than DSVDD on eight datasets, achieving 20%-320% improvement on six datasets, including *donors*, *fuzzers*, *w7a*, *campaign*, *news20* and *thyroid*, and they perform comparably well on the rest of four datasets. PReNet performs significantly better than FSNet and iForest on respective 10 and 12 datasets. In terms of AUC-ROC, PReNet substantially outperforms DevNet, and performs significantly better than DSVDD, FSNet and iForest at the 95% confidence level, with respective 2.9%, 11.7% and 40.7% average improvement.

The superiority of PReNet here is mainly due to that, as discussed in Section 3.1, the pairing data augmentation substantially extends the supervision information of known anomalies through pairwise interaction. As a result, PReNet

Table 2: AUC-PR and AUC-ROC Results (mean \pm std). ‘Size’ is the overall data size, D is the dimension. ‘1M’ denotes *news20* has 1,355,191 features. # wins/draws/losses are counted based on whether the mean \pm std performance of PReNet outperforms/overlaps/underperforms that of its competing methods.

Data Statistics			AUC-PR Performance				
Data	Size	D	PReNet	DevNet	DSVDD	FSNet	iForest
donors	619,326	10	1.000 \pm 0.000	0.997 \pm 0.005	0.806 \pm 0.110	0.995 \pm 0.004	0.222 \pm 0.035
census	299,285	500	0.356 \pm 0.009	0.345 \pm 0.005	0.330 \pm 0.008	0.197 \pm 0.012	0.078 \pm 0.003
fraud	284,807	29	0.689 \pm 0.004	0.693 \pm 0.004	0.695 \pm 0.004	0.157 \pm 0.024	0.261 \pm 0.035
celeba	202,599	39	0.309 \pm 0.004	0.306 \pm 0.014	0.306 \pm 0.006	0.103 \pm 0.015	0.060 \pm 0.007
DoS	109,353	196	0.900 \pm 0.010	0.900 \pm 0.011	0.910 \pm 0.011	0.826 \pm 0.088	0.266 \pm 0.014
reconnaissance	106,987	196	0.767 \pm 0.004	0.760 \pm 0.024	0.772 \pm 0.037	0.650 \pm 0.061	0.132 \pm 0.009
fuzzers	96,000	196	0.170 \pm 0.017	0.136 \pm 0.004	0.133 \pm 0.007	0.146 \pm 0.016	0.039 \pm 0.002
backdoor	95,329	196	0.890 \pm 0.002	0.863 \pm 0.015	0.862 \pm 0.015	0.618 \pm 0.096	0.050 \pm 0.009
w7a	49,749	300	0.496 \pm 0.008	0.408 \pm 0.029	0.117 \pm 0.024	0.098 \pm 0.005	0.023 \pm 0.001
campaign	41,188	62	0.470 \pm 0.008	0.426 \pm 0.008	0.386 \pm 0.014	0.255 \pm 0.017	0.313 \pm 0.022
news20	10,523	1M	0.652 \pm 0.004	0.632 \pm 0.010	0.329 \pm 0.005	0.350 \pm 0.011	0.035 \pm 0.001
thyroid	7,200	21	0.298 \pm 0.008	0.280 \pm 0.006	0.205 \pm 0.007	0.149 \pm 0.016	0.144 \pm 0.019
Average			0.583	0.562	0.488	0.379	0.135
P-value			-	0.005	0.016	0.001	0.001
# wins/draws/losses (PReNet vs.)			-	6/6/0	8/4/0	10/2/0	12/0/0

Data Statistics			AUC-ROC Performance				
Data	Size	D	PReNet	DevNet	DSVDD	FSNet	iForest
donors	619,326	10	1.000 \pm 0.000	1.000 \pm 0.000	0.993 \pm 0.005	0.999 \pm 0.001	0.875 \pm 0.023
census	299,285	500	0.862 \pm 0.003	0.861 \pm 0.002	0.858 \pm 0.005	0.759 \pm 0.007	0.634 \pm 0.015
fraud	284,807	29	0.980 \pm 0.001	0.981 \pm 0.001	0.980 \pm 0.001	0.776 \pm 0.044	0.946 \pm 0.004
celeba	202,599	39	0.960 \pm 0.001	0.961 \pm 0.002	0.958 \pm 0.001	0.855 \pm 0.014	0.686 \pm 0.021
DoS	109,353	196	0.949 \pm 0.007	0.948 \pm 0.007	0.956 \pm 0.005	0.927 \pm 0.019	0.762 \pm 0.018
reconnaissance	106,987	196	0.966 \pm 0.001	0.962 \pm 0.004	0.971 \pm 0.005	0.926 \pm 0.009	0.534 \pm 0.022
fuzzers	96,000	196	0.882 \pm 0.002	0.873 \pm 0.004	0.875 \pm 0.007	0.858 \pm 0.022	0.548 \pm 0.018
backdoor	95,329	196	0.976 \pm 0.002	0.968 \pm 0.006	0.945 \pm 0.018	0.950 \pm 0.018	0.741 \pm 0.039
w7a	49,749	300	0.883 \pm 0.004	0.882 \pm 0.013	0.802 \pm 0.014	0.767 \pm 0.010	0.413 \pm 0.013
campaign	41,188	62	0.880 \pm 0.009	0.858 \pm 0.006	0.803 \pm 0.012	0.684 \pm 0.019	0.723 \pm 0.015
news20	10,523	1M	0.956 \pm 0.004	0.960 \pm 0.001	0.909 \pm 0.002	0.827 \pm 0.009	0.333 \pm 0.012
thyroid	7,200	21	0.781 \pm 0.001	0.767 \pm 0.002	0.713 \pm 0.007	0.590 \pm 0.014	0.679 \pm 0.014
Average			0.923	0.918	0.897	0.827	0.656
P-value			-	0.075	0.025	0.001	0.001
# wins/draws/losses (PReNet vs.)			-	3/9/0	5/7/0	9/3/0	12/0/0

can gain substantial improvement over its contenders when the interaction between $C_{\{a,a\}}/C_{\{a,u\}}/C_{\{u,u\}}$ instance pairs contributes supervision information that cannot be learned using the individual labeled anomaly data. Additionally, the end-to-end anomaly score learning also enables PReNet (as well as DevNet) to make more effective use of the labeled data than the two-step methods DSVDD and FSNet that first feature representations and then calculate anomaly scores based on the new representations.

Note that the performance difference in AUC-PR is far more substantial than that in AUC-ROC in Table 2. This demonstrates the fact that AUC-ROC ignores the detection recall rate of the anomaly class and is considerably less sensitive to the performance of detecting anomalies than AUC-PR, so it shows overoptimistic performance in terms of successfully detecting all anomalies. On the other hand, due to the rareness of anomalies, it is typically very challenging to obtain good AUC-PR performance, *e.g.*, having an AUC-PR performance of greater than 0.7. This explains the large gaps between the average AUC-PR and AUC-ROC results, and also indicates the significance for PReNet to achieve more substantially improved AUC-PR performance than AUC-ROC performance.

4.5 Detection of Unknown Anomalies

Experiment Settings. This section evaluates the generalizability of PReNet in detecting unknown anomalies on the other 28 datasets. Similar to the settings in Section 4.4, the anomaly contamination rate of 2% and $|\mathcal{A}| = 60$ are also used here. The competing method iForest also performs poorly here and is left out for brevity.

Results. The AUC-PR and AUC-ROC performance of PReNet and the three top competing methods on the 28 datasets are presented in Table 3. The results show that PReNet outperforms the three competing methods all by substantial margins in detecting unknown anomalies on the 28 datasets. On average, very impressively, PReNet improves DevNet

by more than 11%, DSVDD by 17% and FSNet by 30% in AUC-PR. It is very encouraging that, compared to the best competing method DevNet, PReNet achieves 20%-130% AUC-PR improvement on eight datasets, including 20%-40% improvement on ‘*reconnaissance → backdoor*’, ‘*reconnaissance, fuzzers → DoS*’, ‘*reconnaissance, backdoor, fuzzers → DoS*’, ‘*backdoor, fuzzers → DoS*’, ‘*fuzzers → DoS*’, ‘*reconnaissance, backdoor, DoS → fuzzers*’, and over 100% improvement on ‘*reconnaissance, fuzzers → backdoor*’ and ‘*fuzzers → backdoor*’. The improvement of PReNet over DSVDD and FSNet is much more substantial than that of PReNet over DevNet, *e.g.*, PReNet gains 21 wins and 6 draws against DSVDD; 25 wins and 3 draws against FSNet. The p-values from the paired *Wilcoxon* signed rank test show that PReNet significantly outperforms all three competing methods at the 99% confidence level. Due to the same reason as in the results of detecting known anomalies in Table 2, the AUC-ROC improvement of PReNet over the competing methods is less than that in the improvement of AUC-PR, but it is also statistically significant at the 99% confidence level, achieving more than 2.5%, 11.1% and 8.0% improvement over DevNet, DSVDD and FSNet, respectively.

These large evaluation results justify the superior improvement of PReNet in generalizing from a few labeled anomalies to detect unknown anomalies. We believe the competing methods may have overfitting of the small labeled anomaly set \mathcal{A} , whereas the substantially augmented data well generalizes PReNet, enabling PReNet to effectively avoid/reduce the potential overfitting. Also, PReNet performs anomaly scoring based on multifaceted representations of both normality and abnormality which are far more expressive than DevNet, DSVDD or FSNet that is built upon single normality, or binary normality and abnormality representations. These unique characteristics make PReNet stand out particularly in complex datasets such as ‘*reconnaissance → backdoor*’, ‘*reconnaissance, fuzzers → backdoor*’, ‘*reconnaissance, fuzzers → DoS*’ and ‘*reconnaissance, backdoor, fuzzers → DoS*’, on which PReNet achieves good/excellent AUC-PR performance against pair/poor AUC-PR performance of all three competing methods. Additionally, due to these characteristics PReNet generally performs more stably than its competing methods as illustrated by its smaller standard deviation of AUC-PR/AUC-ROC results.

DSVDD substantially outperforms PReNet on one out of 28 datasets, ‘*backdoor → DoS*’, on which all detectors obtain excellent AUC-PR performance with DSVDD achieving a nearly perfect AUC-PR result, *i.e.*, an AUC-PR of 0.961. This indicates this dataset is very simple. The availability of a few known backdoor attacks is sufficient to learn an excellent one-class hyperplane detect almost all of the unknown DoS attacks. In such simple cases simpler models like DSVDD and DevNet may be better choices. PReNet also has one lose to DevNet on the dataset ‘*reconnaissance, DoS → fuzzers*’. This may be because the Gaussian prior DevNet makes on the anomaly scores fits this dataset very well, enabling it to learn better anomaly scores than PReNet.

4.6 Availability of Known Anomalies

Experiment Settings. This section examines how effective PReNet can leverage the limited amount of labeled anomaly data by inspecting its performance w.r.t. different number of labeled anomalies, ranging from 15 to 120, with the contamination rate fixed to 2%. The experiments are performed on datasets containing known and unknown anomalies. Since there are too many unknown anomaly datasets to well present all the results, only the results on half of unknown anomaly datasets are reported here. DevNet, DSVDD and FSNet are used as competing methods. The unsupervised method iForest is insensitive to the labeled data and used as the baseline.

Note that since AUC-PR results are much more indicative than AUC-ROC results, we focus on the AUC-PR performance hereafter.

Results. The AUC-PR results on the 12 known anomaly datasets are shown in Fig. 2. The performance of all deep methods generally increases with increasing labeled data. However, the increased anomalies do not always help due to the heterogeneous anomalous behaviors taken by different anomalies. PReNet is more stable in the increasing trend. Consistent to that the results in Table 2, PReNet still significantly outperforms its state-of-the-art competing methods when the availability of known anomalies changes.

Particularly, PReNet demonstrates the most data-efficient learning capability. Impressively, PReNet can be trained with 50%-75% less labeled anomalies but achieves much better, or comparably good, AUC-PR than the best contender DevNet on multiple datasets like *DoS, fuzzers, w7a* and *campaign*; and it is trained with 87.5% less labeled data while obtains substantially better performance than the second best contender DSVDD on *donors, w7a, campaign, news20* and *thyroid*. The same observation applies to FSNet on most of the 12 datasets. We believe the pairing data augmentation is the main driving force for the substantially improved data efficiency of PReNet.

Fig. 3 presents the AUC-PR results on the 14 unknown anomaly datasets. The performance of PReNet here is consistent to that in Table 2. PReNet remains to be the most data-efficient learning method, and can perform substantially better than the best competing methods even when the PReNet model is trained with 50%-87.5% less labeled data.

Table 3: AUC-PR and AUC-ROC Results (mean \pm std) on Detecting Unknown Anomalies. ‘A \rightarrow B’ in the first column means the models are trained with the labeled anomalies A to detect unknown anomalies B. # wins/draws/losses are counted based on whether the mean \pm std performance of PReNet outperforms/overlaps/underperforms that of its competing methods.

Data	AUC-PR Performance			
	PReNet	DevNet	DSVDD	FSNet
Known anomalies \rightarrow Unknown anomalies				
reconnaissance \rightarrow backdoor	0.752 \pm 0.006	0.541 \pm 0.062	0.583 \pm 0.032	0.555 \pm 0.158
reconnaissance, DoS \rightarrow backdoor	0.834 \pm 0.006	0.845 \pm 0.013	0.833 \pm 0.006	0.480 \pm 0.118
reconnaissance, fuzzers \rightarrow backdoor	0.711 \pm 0.014	0.342 \pm 0.065	0.317 \pm 0.102	0.312 \pm 0.088
reconnaissance, DoS, fuzzers \rightarrow backdoor	0.706 \pm 0.016	0.631 \pm 0.033	0.623 \pm 0.034	0.368 \pm 0.166
DoS \rightarrow backdoor	0.908 \pm 0.005	0.908 \pm 0.005	0.890 \pm 0.008	0.772 \pm 0.129
DoS, fuzzers \rightarrow backdoor	0.889 \pm 0.003	0.886 \pm 0.002	0.879 \pm 0.009	0.555 \pm 0.099
fuzzers \rightarrow backdoor	0.503 \pm 0.042	0.219 \pm 0.015	0.266 \pm 0.075	0.466 \pm 0.153
DoS \rightarrow reconnaissance	0.849 \pm 0.012	0.846 \pm 0.016	0.739 \pm 0.017	0.615 \pm 0.048
DoS, fuzzers \rightarrow reconnaissance	0.788 \pm 0.010	0.772 \pm 0.010	0.615 \pm 0.018	0.631 \pm 0.035
DoS, backdoor \rightarrow reconnaissance	0.768 \pm 0.010	0.732 \pm 0.011	0.670 \pm 0.023	0.618 \pm 0.056
DoS, backdoor, fuzzers \rightarrow reconnaissance	0.719 \pm 0.022	0.716 \pm 0.022	0.629 \pm 0.020	0.540 \pm 0.035
backdoor \rightarrow reconnaissance	0.892 \pm 0.012	0.890 \pm 0.016	0.576 \pm 0.069	0.689 \pm 0.049
backdoor, fuzzers \rightarrow reconnaissance	0.876 \pm 0.004	0.804 \pm 0.042	0.831 \pm 0.031	0.672 \pm 0.065
fuzzers \rightarrow reconnaissance	0.797 \pm 0.022	0.718 \pm 0.042	0.727 \pm 0.060	0.760 \pm 0.045
reconnaissance \rightarrow DoS	0.928 \pm 0.002	0.846 \pm 0.012	0.855 \pm 0.010	0.798 \pm 0.062
reconnaissance, fuzzers \rightarrow DoS	0.883 \pm 0.004	0.718 \pm 0.030	0.673 \pm 0.039	0.670 \pm 0.096
reconnaissance, backdoor \rightarrow DoS	0.891 \pm 0.008	0.870 \pm 0.016	0.871 \pm 0.013	0.686 \pm 0.067
reconnaissance, backdoor, fuzzers \rightarrow DoS	0.835 \pm 0.007	0.610 \pm 0.036	0.699 \pm 0.053	0.572 \pm 0.066
backdoor \rightarrow DoS	0.938 \pm 0.012	0.943 \pm 0.011	0.961 \pm 0.008	0.930 \pm 0.013
backdoor, fuzzers \rightarrow DoS	0.932 \pm 0.001	0.761 \pm 0.031	0.772 \pm 0.028	0.714 \pm 0.092
fuzzers \rightarrow DoS	0.811 \pm 0.007	0.644 \pm 0.040	0.680 \pm 0.074	0.774 \pm 0.055
reconnaissance \rightarrow fuzzers	0.462 \pm 0.003	0.418 \pm 0.014	0.419 \pm 0.008	0.410 \pm 0.032
reconnaissance, DoS \rightarrow fuzzers	0.349 \pm 0.012	0.375 \pm 0.007	0.366 \pm 0.014	0.276 \pm 0.030
reconnaissance, backdoor \rightarrow fuzzers	0.315 \pm 0.005	0.311 \pm 0.013	0.314 \pm 0.009	0.260 \pm 0.025
reconnaissance, backdoor, DoS \rightarrow fuzzers	0.294 \pm 0.006	0.246 \pm 0.004	0.249 \pm 0.001	0.206 \pm 0.024
DoS \rightarrow fuzzers	0.418 \pm 0.014	0.427 \pm 0.026	0.325 \pm 0.020	0.288 \pm 0.037
DoS, backdoor \rightarrow fuzzers	0.375 \pm 0.007	0.371 \pm 0.008	0.322 \pm 0.016	0.273 \pm 0.021
backdoor \rightarrow fuzzers	0.418 \pm 0.008	0.420 \pm 0.017	0.250 \pm 0.011	0.374 \pm 0.030
Average	0.709	0.636	0.605	0.545
P-value	-	0.001	0.000	0.000
# wins/draws/losses (PReNet vs.)	-	14/13/1	21/6/1	25/3/0

Data	AUC-ROC Performance			
	PReNet	DevNet	DSVDD	FSNet
Known anomalies \rightarrow Unknown anomalies				
reconnaissance \rightarrow backdoor	0.965 \pm 0.000	0.900 \pm 0.012	0.902 \pm 0.013	0.885 \pm 0.063
reconnaissance, DoS \rightarrow backdoor	0.977 \pm 0.002	0.980 \pm 0.002	0.978 \pm 0.001	0.924 \pm 0.016
reconnaissance, fuzzers \rightarrow backdoor	0.969 \pm 0.001	0.891 \pm 0.010	0.890 \pm 0.021	0.865 \pm 0.024
reconnaissance, DoS, fuzzers \rightarrow backdoor	0.971 \pm 0.002	0.953 \pm 0.008	0.952 \pm 0.017	0.916 \pm 0.030
DoS \rightarrow backdoor	0.958 \pm 0.002	0.956 \pm 0.006	0.924 \pm 0.010	0.932 \pm 0.021
DoS, fuzzers \rightarrow backdoor	0.969 \pm 0.003	0.967 \pm 0.004	0.918 \pm 0.011	0.921 \pm 0.016
fuzzers \rightarrow backdoor	0.869 \pm 0.004	0.794 \pm 0.009	0.812 \pm 0.029	0.872 \pm 0.050
DoS \rightarrow reconnaissance	0.867 \pm 0.018	0.865 \pm 0.025	0.677 \pm 0.030	0.636 \pm 0.083
DoS, fuzzers \rightarrow reconnaissance	0.899 \pm 0.013	0.885 \pm 0.011	0.663 \pm 0.026	0.842 \pm 0.037
DoS, backdoor \rightarrow reconnaissance	0.908 \pm 0.008	0.891 \pm 0.005	0.724 \pm 0.037	0.859 \pm 0.035
DoS, backdoor, fuzzers \rightarrow reconnaissance	0.907 \pm 0.005	0.907 \pm 0.007	0.820 \pm 0.039	0.871 \pm 0.014
backdoor \rightarrow reconnaissance	0.928 \pm 0.007	0.926 \pm 0.014	0.489 \pm 0.099	0.693 \pm 0.096
backdoor, fuzzers \rightarrow reconnaissance	0.958 \pm 0.002	0.943 \pm 0.011	0.947 \pm 0.009	0.879 \pm 0.017
fuzzers \rightarrow reconnaissance	0.890 \pm 0.008	0.855 \pm 0.021	0.863 \pm 0.023	0.871 \pm 0.031
reconnaissance \rightarrow DoS	0.938 \pm 0.002	0.883 \pm 0.008	0.887 \pm 0.006	0.825 \pm 0.037
reconnaissance, fuzzers \rightarrow DoS	0.939 \pm 0.001	0.874 \pm 0.011	0.868 \pm 0.010	0.834 \pm 0.043
reconnaissance, backdoor \rightarrow DoS	0.944 \pm 0.003	0.932 \pm 0.006	0.931 \pm 0.005	0.872 \pm 0.029
reconnaissance, backdoor, fuzzers \rightarrow DoS	0.940 \pm 0.002	0.861 \pm 0.008	0.886 \pm 0.023	0.821 \pm 0.021
backdoor \rightarrow DoS	0.906 \pm 0.024	0.915 \pm 0.021	0.945 \pm 0.011	0.926 \pm 0.013
backdoor, fuzzers \rightarrow DoS	0.958 \pm 0.000	0.889 \pm 0.013	0.887 \pm 0.014	0.872 \pm 0.033
fuzzers \rightarrow DoS	0.855 \pm 0.002	0.792 \pm 0.018	0.805 \pm 0.028	0.826 \pm 0.037
reconnaissance \rightarrow fuzzers	0.878 \pm 0.005	0.872 \pm 0.001	0.872 \pm 0.002	0.843 \pm 0.023
reconnaissance, DoS \rightarrow fuzzers	0.850 \pm 0.014	0.889 \pm 0.005	0.871 \pm 0.028	0.822 \pm 0.021
reconnaissance, backdoor \rightarrow fuzzers	0.879 \pm 0.006	0.879 \pm 0.001	0.880 \pm 0.002	0.838 \pm 0.034
reconnaissance, backdoor, DoS \rightarrow fuzzers	0.885 \pm 0.002	0.878 \pm 0.001	0.878 \pm 0.001	0.846 \pm 0.018
DoS \rightarrow fuzzers	0.708 \pm 0.030	0.737 \pm 0.049	0.508 \pm 0.045	0.606 \pm 0.094
DoS, backdoor \rightarrow fuzzers	0.842 \pm 0.012	0.833 \pm 0.010	0.646 \pm 0.065	0.837 \pm 0.029
backdoor \rightarrow fuzzers	0.752 \pm 0.014	0.743 \pm 0.030	0.364 \pm 0.059	0.697 \pm 0.072
Average	0.904	0.882	0.814	0.837
P-value	-	0.001	0.000	0.000
# wins/draws/losses (PReNet vs.)	-	14/13/1	20/7/1	18/10/0

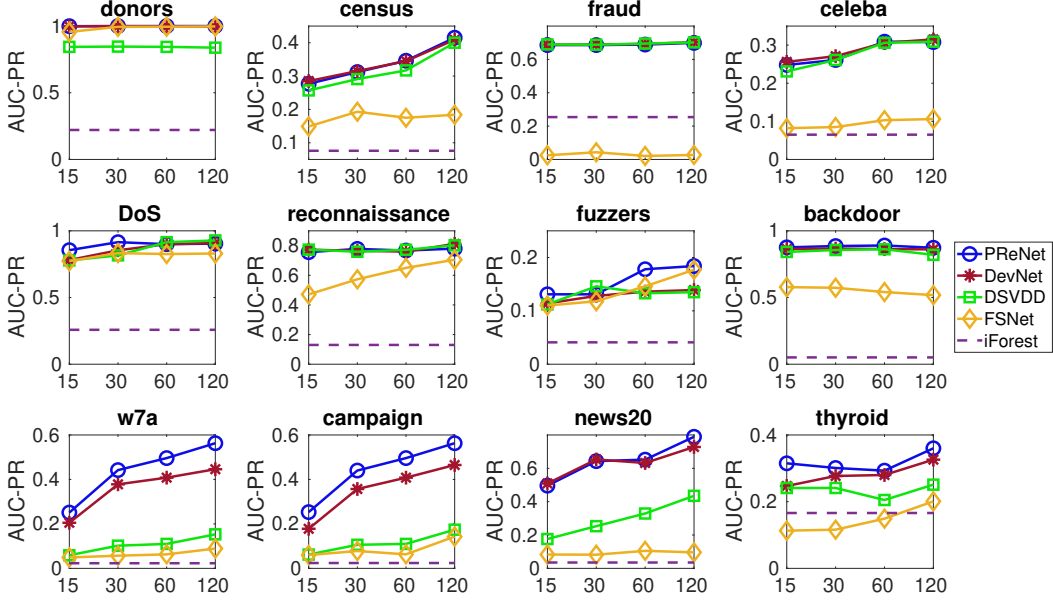


Figure 2: AUC-PR Performance w.r.t. the Number of Labeled Anomalies

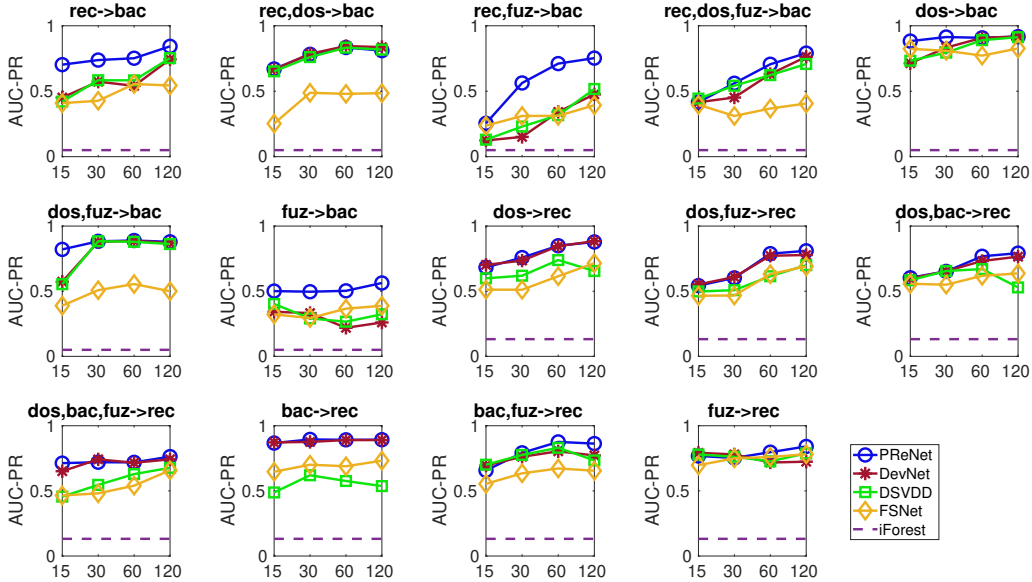


Figure 3: AUC-PR Performance of Detecting Unknown Anomalies Using Different Number of Labeled Anomalies. ‘rec’, ‘bac’, ‘dos’ and ‘fuz’ respectively present the attacks ‘reconnaissance’, ‘backdoor’, ‘DoS’ and ‘fuzzers’. ‘A -> B’ means that the models are trained with labeled attacks ‘A’ to detect unknown attacks ‘B’.

4.7 Further Analysis of PReNet

This section inspects some intrinsic behaviors of PReNet. Since the findings on the known and unknown anomaly datasets are similar, here we focus on the 12 known anomaly datasets.

4.7.1 Tolerance to Anomaly Contamination in Unlabeled Data

Experiment Settings. We examine the robustness w.r.t. different anomaly contamination rates, {0%, 2%, 5%, 10%}, with the number of labeled anomalies fixed to 60. The case with 0% contamination rate is used as the baseline.

Results. The AUC-PR results of PReNet w.r.t. different contamination rates are presented in Fig. 4. As expected in our theoretical analysis in Section 3.2, PReNet performs very well and stably on all datasets when the contamination rate is reasonably small, *e.g.*, 2%-5%. It is very impressive that this trend remains on nearly all datasets except *census*, *w7a* and *news20*, even when the rate increases to 10%. This robustness is due to two main reasons: (i) the regression modeling itself is tolerant to a certain proportion of outliers, and (ii) our theoretical analysis suggests that in PReNet true anomalies are expected to be assigned with larger anomaly scores than normal instances for small anomaly contamination.

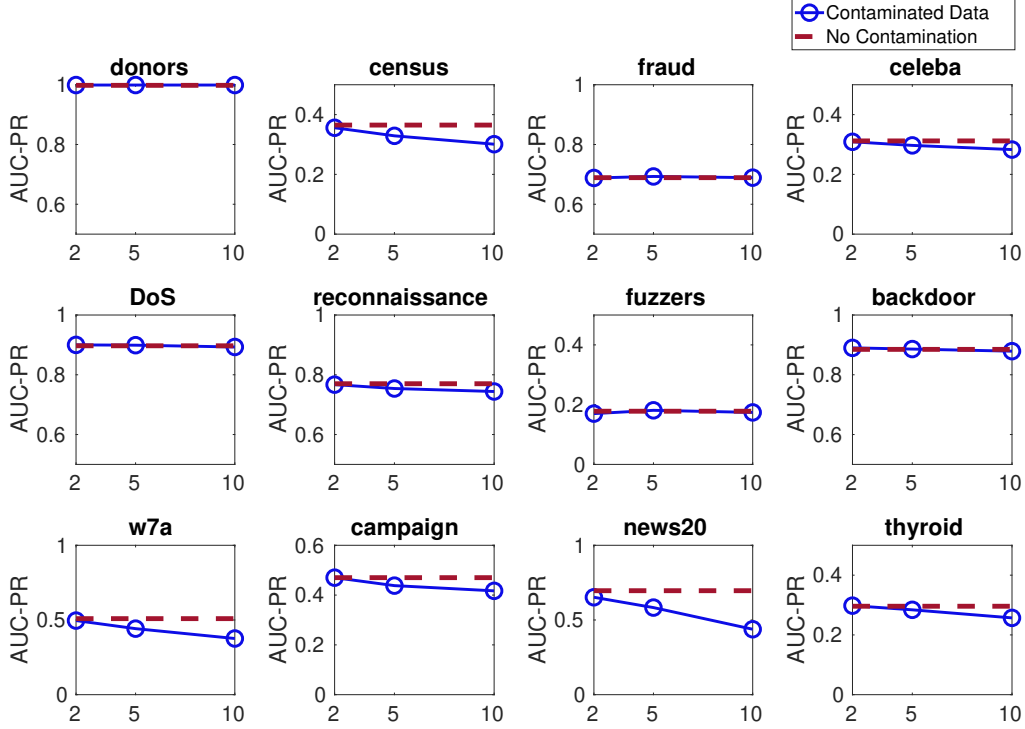


Figure 4: AUC-PR Performance of PReNet on Data of Different Contamination Rates (%). The PReNet’s performance on data with no anomaly contamination is used as the baseline.

4.7.2 Ablation Study

Experiment Settings. PReNet is compared with the following four ablated variants to examine the importance of its key individual components:

- **BOR.** BOR reduces PReNet from ternary ordinal regression to Binary Ordinal Regression (BOR) by merging the two anomaly-related synthetic class labels $y_{\{a,a\}} = 8$ and $y_{\{a,u\}} = 4$ into one label $y_{\{a,a\}|\{a,u\}} = 4$, with the class $y_{\{u,u\}} = 0$ unchanged.
- **OSNet.** OSNet is a simplified PReNet that is reduced from a two-stream neural network to a One-Stream neural Network (OSNet), which means OSNet takes single data points as inputs rather than pairs of data points in PReNet. In other words, OSNet discards the pairing-based data augmentation in PReNet. Also, for single data points, we can only have two possible synthetic class labels y_a and y_u . Therefore, OSNet trains a binary ordinal regression model with $y_a = 4$ and $y_u = 0$.
- **LDM.** LDM removes the hidden layers of PReNet and learns a Linear Direct Mapping (LDM) from the original data space to anomaly scores.
- **A2H.** A2H is a variant having more complex network architecture than PReNet, which deepens PReNet with additional two hidden (A2H) layers. ℓ_2 -norm regularizer is also added to these hidden layers to avoid overfitting.

Results. The ablation study results are shown in Table 4. The results show that PReNet performs substantially better than its four variants by large improvement margins, *i.e.*, BOR (5.6%), OSNet (3.7%), LDM (11.0%) and A2H (3.3%). The improvement over BOR and OSNet are statistically significant at the 99% confidence level. This justifies that both

of the pairing data augmentation and ternary ordinal regression makes significant contribution to the performance of PReNet. On the other hand, it is impressive that even BOR and OSNet are the simplified variants of PReNet, they perform comparably well to the best state-of-the-art competing method DevNet in Table 2. Eliminating the feature representation layer, *i.e.*, the ψ function, from PReNet results in LDM, which also performs significantly worse than PReNet, with over 10% loss in the average AUC-PR performance, indicating the critical role of the intermediate representation learning in PReNet. Compared to the variant with a deeper architecture, A2H, although PReNet achieves large average improvement, the improvement is not statistically significant across the datasets. This is because the deeper architecture can help achieve significant AUC-PR gains on some datasets like *reconnaissance* and *thyroid*, but significantly deteriorates on most of the other datasets. Thus, the default network architecture used in PReNet is generally recommended.

Table 4: AUC-PR Performance of PReNet and Its Four Ablated Variants.

Data	PReNet	BOR	OSNet	LDM	A2H
donors	1.000 \pm 0.000	0.995 \pm 0.011	0.999 \pm 0.002	0.974 \pm 0.023	1.000 \pm 0.000
census	0.356 \pm 0.009	0.324 \pm 0.010	0.325 \pm 0.011	0.355 \pm 0.001	0.283 \pm 0.035
fraud	0.689 \pm 0.004	0.692 \pm 0.008	0.701 \pm 0.008	0.662 \pm 0.004	0.708 \pm 0.004
celeba	0.309 \pm 0.004	0.308 \pm 0.007	0.299 \pm 0.016	0.294 \pm 0.005	0.299 \pm 0.007
DoS	0.900 \pm 0.010	0.887 \pm 0.003	0.887 \pm 0.005	0.839 \pm 0.003	0.877 \pm 0.015
reconnaissance	0.767 \pm 0.004	0.751 \pm 0.016	0.750 \pm 0.015	0.647 \pm 0.005	0.877 \pm 0.005
fuzzers	0.170 \pm 0.017	0.147 \pm 0.009	0.151 \pm 0.008	0.163 \pm 0.004	0.178 \pm 0.015
backdoor	0.890 \pm 0.002	0.879 \pm 0.006	0.879 \pm 0.007	0.805 \pm 0.012	0.863 \pm 0.008
w7a	0.496 \pm 0.008	0.467 \pm 0.015	0.482 \pm 0.011	0.406 \pm 0.002	0.415 \pm 0.016
campaign	0.470 \pm 0.008	0.423 \pm 0.010	0.402 \pm 0.010	0.406 \pm 0.003	0.246 \pm 0.042
news20	0.652 \pm 0.004	0.481 \pm 0.004	0.625 \pm 0.004	0.552 \pm 0.001	0.618 \pm 0.023
thyroid	0.298 \pm 0.008	0.269 \pm 0.013	0.248 \pm 0.011	0.201 \pm 0.015	0.411 \pm 0.015
Average	0.583	0.552	0.562	0.525	0.565
P-value	-	0.002	0.003	0.001	0.413

5 Related Work

5.1 Deep Anomaly Detection

Traditional anomaly detection approaches are often ineffective in high-dimensional or non-linear separable data due to the curse of dimensionality and the deficiency in capturing the non-linear relations [13]. Deep anomaly detection has shown promising results in handle those complex data, of which most methods are based on autoencoders [32, 6] or generative adversarial networks [7, 8]. These methods generally follow a two-step approach. They often first learn new representations of the data and use the reconstruction loss from the new representation space as anomaly score. One issue with these methods is that the learned representations are primarily optimized to represent the whole data rather than to detect anomalies. Some very recent methods [33, 9, 10, 12] address this issue by learning representations tailored for specific anomaly measures, *e.g.* cluster membership-based measure in [33], distance-based measure in [9] and one-class classification-based measure in [10, 12, 34]. However, they still focus on optimizing the feature representations. By contrast, PReNet unifies representation learning and anomaly scoring into one pipeline to directly optimize anomaly scores, yielding more optimized anomaly scores.

5.2 Weakly- and Semi-supervised Anomaly Detection

Many studies have been introduced to leverage labeled normal instances to learn patterns of the normal class, which are commonly referred to as semi-supervised anomaly detection methods [18, 19, 20]. The semi-supervised setting is relevant to our problem because of the availability of both labeled and unlabeled data, but they are two fundamentally different tasks due to the difference in training data and the problem nature. Specifically, we have only a few labeled anomaly data rather than large-scale labeled normal data; and the anomalies are often from different distributions or manifolds, so having only limited labeled anomaly data hardly cover all types of anomalies. Therefore, instead of modeling the labeled normal data, our problem requires to learn patterns of labeled anomalies that also generalize well to unseen anomalies. A few studies [14, 15, 16, 9] show that these limited labeled anomalies can be leveraged to substantially improve the detection accuracy. However, these studies exploit the labeled anomalies to enhance anomaly scoring via label propagation [14, 15], representation learning [9] or classification models [16], failing to sufficiently utilize the labeled data and/or detect unseen anomalies. [34] studies a partly similar problem to ours. One key difference is that a small set of both labeled anomalies and normal instances are assumed to be available in [34], while we only assume the availability of a few labeled anomalies. They address the problem by extending DSVDD with an additional

term into the SVDD objective function to guarantee the large (small) margin between the one-class center and labeled anomalies (normal instances). The adaptive DSVDD used in our comparison shares a similar spirit to this extended DSVDD.

This research line is also relevant to few-shot classification [35, 36, 29] and positive and unlabeled data (PU) learning [37, 38, 39] because of the availability of the limited labeled positive instances (anomalies), but they are very different in that these two areas implicitly assume that the few labeled instances share the same intrinsic class structure as the other instances within the same class (e.g., the anomaly class), whereas the few labeled anomalies and the unknown anomalies may have diverse class structures. This presents significant challenges to the techniques of both areas.

Our previous work DevNet [11] addresses the same problem as this work, but is a completely different approach to our approach in this study. Here we formulate the problem as a pairwise relation learning task and address the problem using deep ternary ordinal regression with no strong assumption on data distribution or anomaly scores, whereas DevNet assumes the anomaly scores of data instances follow a Gaussian distribution and leverages this prior to learn the anomaly scores by fitting to a Z-Score-based distribution. The resulting PReNet achieves significantly better performance than DevNet in detecting both known and unknown anomalies, and is also substantially more data-efficient.

6 Conclusions and Discussions

This paper introduces a novel formulation and its instantiation to devise two-stream ordinal regression neural networks for deep weakly-supervised anomaly detection. Our approach achieves significant improvement over four state-of-the-art competing methods in detecting both known and unknown anomalies and data efficiency. This well justifies our approach’s capability in generalizing from a few labeled anomalies and its tolerance to anomaly contamination in the unlabeled data. Particularly, our significantly improved precision-recall performance in unknown anomaly detection, *i.e.*, 10%-30%, is very encourage in that (i) it is already very challenging to improve this metric for known anomalies, and the challenge is further largely increased for the unknown anomalies; and (ii) detecting unknown anomalies is one of the most critical open problems and of tremendous interest in numerous real-world applications. Our results may suggest the labeled anomaly data, regardless of its scale, should be fully leveraged to enable more accurate and comprehensive anomaly detection.

The proposed technique may be further improved to consider, beyond pairwise, listwise relation. Though our preliminary experiments (results not shown in the paper) found PReNet is not sensitive to the relation values of c_1 to c_3 , some further investigation there may help improve the detection performance.

References

- [1] Markus M Breunig, Hans-Peter Kriegel, Raymond T Ng, and Jörg Sander. LOF: Identifying density-based local outliers. In *ACM Sigmod Record*, volume 29, pages 93–104. ACM, 2000.
- [2] Hans-Peter Kriegel, Matthias Schubert, and Arthur Zimek. Angle-based outlier detection in high-dimensional data. In *KDD*, pages 444–452. ACM, 2008.
- [3] Ke Zhang, Marcus Hutter, and Huidong Jin. A new local distance-based outlier detection approach for scattered real-world data. In *PAKDD*, pages 813–822. Springer, 2009.
- [4] Huidong Jin, Jie Chen, Hongxing He, Chris Kelman, Damien McAullay, and Christine M O’Keefe. Signaling potential adverse drug reactions from administrative health databases. *IEEE Transactions on Knowledge and Data Engineering*, 22(6):839–853, 2010.
- [5] Fei Tony Liu, Kai Ming Ting, and Zhi-Hua Zhou. Isolation-based anomaly detection. *ACM Transactions on Knowledge Discovery from Data*, 6(1):3, 2012.
- [6] Jinghui Chen, Saket Sathé, Charu Aggarwal, and Deepak Turaga. Outlier detection with autoencoder ensembles. In *SDM*, pages 90–98. SIAM, 2017.
- [7] Thomas Schlegl, Philipp Seeböck, Sebastian M Waldstein, Ursula Schmidt-Erfurth, and Georg Langs. Unsupervised anomaly detection with generative adversarial networks to guide marker discovery. In *IPMI*, pages 146–157. Springer, Cham, 2017.
- [8] Houssam Zenati, Manon Romain, Chuan-Sheng Foo, Bruno Lecouat, and Vijay Chandrasekhar. Adversarially learned anomaly detection. In *ICDM*, pages 727–736. IEEE, 2018.
- [9] Guansong Pang, Longbing Cao, Ling Chen, and Huan Liu. Learning representations of ultrahigh-dimensional data for random distance-based outlier detection. In *KDD*, pages 2041–2050, 2018.

- [10] Lukas Ruff, Nico Görnitz, Lucas Deecke, Shoaib Ahmed Siddiqui, Robert Vandermeulen, Alexander Binder, Emmanuel Müller, and Marius Kloft. Deep one-class classification. In *ICML*, pages 4390–4399, 2018.
- [11] Guansong Pang, Chunhua Shen, and Anton van den Hengel. Deep anomaly detection with deviation networks. In *KDD*, pages 353–362. ACM, 2019.
- [12] Panpan Zheng, Shuhan Yuan, Xintao Wu, Jun Li, and Aidong Lu. One-class adversarial nets for fraud detection. In *AAAI*, volume 33, pages 1286–1293, 2019.
- [13] Charu C Aggarwal. *Outlier analysis*. Springer, 2017.
- [14] Mary McGlohon, Stephen Bay, Markus G Anderle, David M Steier, and Christos Faloutsos. SNARE: A link analytic system for graph labeling and risk detection. In *KDD*, pages 1265–1274. ACM, 2009.
- [15] Acar Tamersoy, Kevin Roundy, and Duen Horng Chau. Guilt by association: Large scale malware detection by mining file-relation graphs. In *KDD*, pages 1524–1533, 2014.
- [16] Ya-Lin Zhang, Longfei Li, Jun Zhou, Xiaolong Li, and Zhi-Hua Zhou. Anomaly detection with partially observed anomalies. In *WWW Companion*, pages 639–646, 2018.
- [17] Ian Goodfellow, Yoshua Bengio, and Aaron Courville. *Deep learning*. MIT press, 2016.
- [18] Keith Noto, Carla Brodley, and Donna Slonim. FRaC: a feature-modeling approach for semi-supervised and unsupervised anomaly detection. *Data Mining and Knowledge Discovery*, 25(1):109–133, 2012.
- [19] Nico Görnitz, Marius Kloft, Konrad Rieck, and Ulf Brefeld. Toward supervised anomaly detection. *Journal of Artificial Intelligence Research*, 46:235–262, 2013.
- [20] Dino Ienco, Ruggero G Pensa, and Rosa Meo. A semisupervised approach to the detection and characterization of outliers in categorical data. *IEEE Transactions on Neural Networks and Learning Systems*, 28(5):1017–1029, 2017.
- [21] Xiang Zhang and Yann LeCun. Text understanding from scratch. *arXiv preprint:1502.01710*, 2015.
- [22] Luis Perez and Jason Wang. The effectiveness of data augmentation in image classification using deep learning. *arXiv preprint:1712.04621*, 2017.
- [23] Xavier Glorot and Yoshua Bengio. Understanding the difficulty of training deep feedforward neural networks. In *AISTATS*, pages 249–256, 2010.
- [24] Yiyuan She and Art B Owen. Outlier detection using nonconvex penalized regression. *Journal of the American Statistical Association*, 106(494):626–639, 2011.
- [25] Chun Yu and Weixin Yao. Robust linear regression: A review and comparison. *Communications in Statistics-Simulation and Computation*, 46(8):6261–6282, 2017.
- [26] Nour Moustafa and Jill Slay. UNSW-NB15: a comprehensive data set for network intrusion detection systems. In *Military Communications and Information Systems Conference, 2015*, pages 1–6, 2015.
- [27] Arthur Zimek, Matthew Gaudet, Ricardo JGB Campello, and Jörg Sander. Subsampling for efficient and effective unsupervised outlier detection ensembles. In *KDD*, pages 428–436. ACM, 2013.
- [28] David MJ Tax and Robert PW Duin. Support vector data description. *Machine Learning*, 54(1):45–66, 2004.
- [29] Jake Snell, Kevin Swersky, and Richard Zemel. Prototypical networks for few-shot learning. In *NIPS*, pages 4077–4087, 2017.
- [30] Kendrick Boyd, Kevin H Eng, and C David Page. Area under the precision-recall curve: point estimates and confidence intervals. In *ECML/PKDD*, pages 451–466. Springer, 2013.
- [31] RF Woolson. Wilcoxon signed-rank test. *Wiley Encyclopedia of Clinical Trials*, pages 1–3, 2007.
- [32] Simon Hawkins, Hongxing He, Graham Williams, and Rohan Baxter. Outlier detection using replicator neural networks. In *DaWaK*, 2002.
- [33] Bo Zong, Qi Song, Martin Renqiang Min, Wei Cheng, Cristian Lumezanu, Daeki Cho, and Haifeng Chen. Deep autoencoding gaussian mixture model for unsupervised anomaly detection. In *ICLR*, 2018.
- [34] Lukas Ruff, Robert A Vandermeulen, Nico Görnitz, Alexander Binder, Emmanuel Müller, Klaus-Robert Müller, and Marius Kloft. Deep semi-supervised anomaly detection. *arXiv preprint arXiv:1906.02694*, 2019.
- [35] Li Fei-Fei, Rob Fergus, and Pietro Perona. One-shot learning of object categories. *IEEE Transactions on Pattern Analysis and Machine Intelligence*, 28(4):594–611, 2006.
- [36] Oriol Vinyals, Charles Blundell, Timothy Lillicrap, Daan Wierstra, et al. Matching networks for one shot learning. In *NIPS*, pages 3630–3638, 2016.

- [37] Xiaoli Li and Bing Liu. Learning to classify texts using positive and unlabeled data. In *IJCAI*, volume 3, pages 587–592, 2003.
- [38] Charles Elkan and Keith Noto. Learning classifiers from only positive and unlabeled data. In *KDD*, pages 213–220. ACM, 2008.
- [39] Emanuele Sansone, Francesco GB De Natale, and Zhi-Hua Zhou. Efficient training for positive unlabeled learning. *IEEE Transactions on Pattern Analysis and Machine Intelligence*, 2018.